Adsorption of a model protein, the GroEL chaperonin, on surfaces

2008 J. Phys.: Condens. Matter 20 353001

(http://iopscience.iop.org/0953-8984/20/35/353001)

IOP PUBLISHING JOURNAL OF PHYSICS: CONDENSED MATTER

J. Phys.: Condens. Matter **20** (2008) 353001 (10pp) doi:10.1088/0953-8984/20/35/353001

TOPICAL REVIEW

Adsorption of a model protein, the GroEL chaperonin, on surfaces

Carl Leung[1] **and Richard E Palmer**

Nanoscale Physics Research Laboratory, School of Physics and Astronomy, The University of Birmingham, Edgbaston, Birmingham B15 2TT, UK

E-mail: carl.leung@kcl.ac.uk

Received 9 June 2008
Published 12 August 2008
Online at stacks.iop.org/JPhysCM/20/353001

Abstract

Understanding and controlling protein adsorption on surfaces is fundamental to many biological processes ranging from cell adhesion to the fabrication of protein biochips. In general, proteins need to retain their 3D conformation to perform their intended functions. However, when they are presented with a solid surface, complex interactions ranging from weak non-covalent binding to strong covalent bonding may occur, which can potentially induce conformational changes within the adsorbed protein. To investigate the surface adsorption process and its effects on a model protein, the chaperonin GroEL, we have applied contact mode atomic force microscopy, in buffer solution to probe the interactions between single proteins and surfaces in real space. We will discuss the adsorption of GroEL molecules on planar surfaces (mica, graphite and gold) and specifically tailored nanostructured surfaces, which present structural features on the size scale of individual biological molecules.

(Some figures in this article are in colour only in the electronic version)

Contents

[1] Author to whom any correspondence should be addressed. Present address: Division of Engineering, King's College London, Strand, London, WC2R 2LS, UK.

1. Introduction

Chaperonins are proteins that guide other proteins along the proper pathways for folding. The chaperonin complex of the bacterium *E.coli* is constructed from two component parts, GroEL (molecular weight $M_w = 58\,000$) and GroES ($M_w = 10\,000$). The active complex contains 14 copies of GroEL and seven copies of GroES, giving a total M_w of about 900 000. In the absence of GroES, the 14 GroEL molecules form two sevenfold rings packed back to back [1, 2]. Each ring surrounds a cavity open at one end to receive misfolded proteins and the two rings communicate with each other via allosteric structural changes which are important to the mechanism of the chaperonin. From the top view, the GroEL ring is 14 nm wide with a protein-sized cavity of about 5 nm in diameter (figure 1). Furthermore, the GroEL ring is highly flexible and is capable of undergoing very large conformational changes [2]. The ring shape and the function of the GroEL therefore makes it an attractive model protein for probing by surface science techniques such as atomic force microscopy (AFM). In principle, the AFM is capable of probing, in real space and

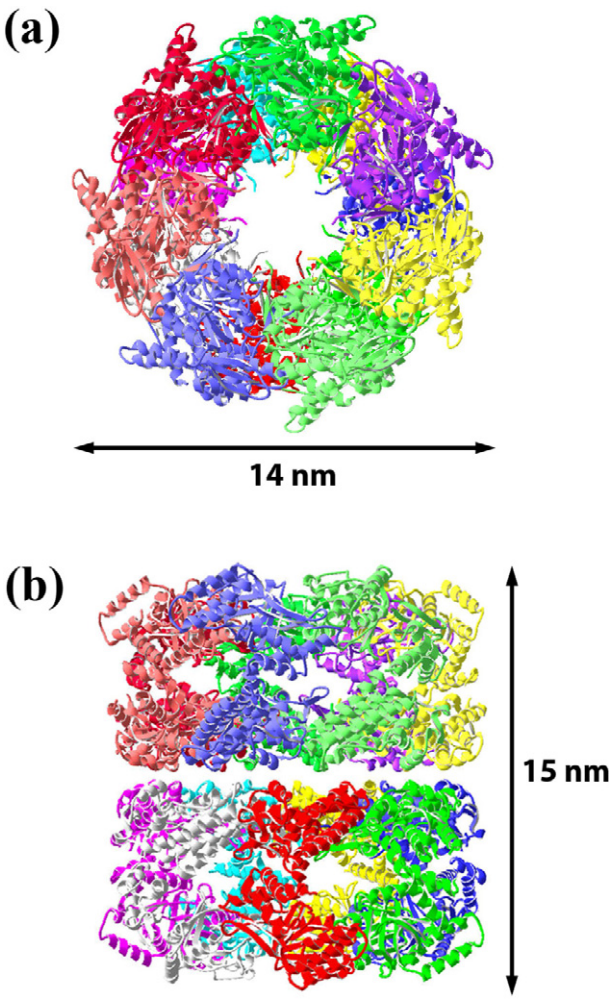

Figure 1. The GroEL complex. (a) Ribbon representation of the GroEL complex from above. The large internal cavity allows a protein chain trapped inside (not shown) to fold on its own. (b) A ribbon schematic of the unbound GroEL ring with each constituent chain coloured differently. The schematic is generated from x-ray crystallographic data using Deepview [42]. The molecule is about 14 nm across, 15 nm in height with the central cavity being approximately 5 nm.

in real time, a single isolated protein molecule (i.e. free from the influence of other neighbouring proteins) in buffer solution. The impetus for studying a single, isolated protein molecule is to provide, ultimately, valuable information on structural conformational changes as the protein performs its function in a near native environment.

Extended surfaces which are designed to preserve the conformation and biological activity of proteins can be rapidly contaminated when exposed to ambient air and therefore they need to be prepared or activated immediately before use. Some model extended surfaces for AFM imaging include mica and graphite (e.g. highly oriented pyrolytic graphite, HOPG), which can both be cleaved to reveal a fresh surface layer before use. For AFM studies of large biological molecules, e.g. proteins, the smooth and unreactive surface of graphite often makes for a model hydrophobic substrate [3–6] as compared to the more hydrophilic mica. The hydrophobic nature of graphite can also be advantageously employed to immobilize proteins containing large hydrophobic patches such as fibrinogen [5]. Mica has proven to be an excellent solid support for AFM studies; DNA [7], membrane proteins [8], cells [9] and virus particles [10] are amongst the biological entities to be physisorbed and analysed on a bare mica surface. Since mica carries an overall negative charge, molecules carrying the same charge (e.g. DNA) are less susceptible to adsorption. To counteract this effect, the mica can be exposed to a solution of divalent cations (usually magnesium or nickel) and such a pre-treatment procedure can be beneficial for AFM imaging of e.g., ocular mucins [11, 12] and actin filaments [13] in air or in aqueous environments.

In the literature mica is also the preferred substrate for GroEL imaging. For instance, Valle *et al* [14, 15] achieved the necessary immobilization simply by allowing time for GroEL to adsorb from solution onto a freshly cleaved hydrophilic mica substrate. Adsorption was improved by increasing the concentration of electrolytes in the imaging buffer such that the GroEL film was stable even after repeated tapping mode scans in the same area. Mou *et al* [16, 17] employed glutaraldehyde as a fixation agent for imaging GroEL on mica. Glutaraldehyde fixation of the chaperonin improved the stability of the image such that all seven subunits of the GroEL ring could be resolved; however, the biological activity of the GroEL was destroyed by the chemical fixation step. More recently, using a mutated single ring GroEL, Schiener *et al* [18] showed that the protein binds with different orientations depending on the hydrophobic/hydrophilic nature of the surface.

While the reported AFM imaging of the GroEL ring usually involves the use of fixatives to immobilize the protein for high resolution imaging [17], the resolution achieved is still lower than other biological samples, such as reconstituted membrane proteins [19]. The major limitation for high resolution imaging of GroEL is the problem of bisection of the protein by the scanning tip due to the weak inter-ring contacts [14, 15, 18]. Furthermore, most protein AFM experiments are carried out in tapping mode which provides little or no information about the protein-surface interaction. In this study, all AFM images are collected in contact mode, providing a qualitative measure of the strength of the protein adsorption on the surface.

2. Experimental section

2.1. AFM instrumentation

A dimension 3100 scanning probe microscope (Veeco, California) with a Nanoscope IIIa controller was used for imaging GroEL in aqueous environments. Imaging was performed in contact mode. The cantilevers used are commercially available from Olympus, Japan. A typical cantilever for the protein imaging experiments will have a spring constant of 0.09 N m^{-1}, a tip radius of about 20 nm and a reflective gold plating on the back side of the cantilever. Tips were cleaned by rinsing with distilled water followed by the buffer solution before usage. In aqueous environments, an all glass, transparent fluid cell with a flexible skirt seal was

necessary to prevent ingress of liquid into the piezoelectric elements.

With the sample to be analysed already immersed in buffer solution, the cantilever is slowly lowered into the liquid until a deflection corresponding to contact between the tip and the sample is registered. This initial contact force is usually sufficient to disrupt any soft biological matter such as proteins, and for this reason a very small area (typically 2 nm square) is chosen as the initial contact scan area to minimize damage by the scanning tip. The contact force is gradually lowered until the tip just loses contact with the surface, and then increased again to about 0.5 nN. When this balance has been achieved, the tip is raster-scanned over larger areas of the sample, and other parameters such as the integral gain, proportional gain, and scan speed are adjusted. Ultrapure water in 50 μl amounts is pipetted about every half an hour to minimize the effects of evaporation. For the *in situ* experiments involving electrolytes, the substrate is mounted in a petri dish and immersed into the appropriate buffer solution.

All experiments were performed at room temperature, and the images were collected at the maximum 512 × 512 pixels allowable by the controller and the Nanoscope software. No image processing was performed on the raw data except for a first order flattening using Image SXM [20].

2.2. Scanning tunnelling microscopy

The STM module is operated through a Nanoscope IIIa AFM controller (Veeco, California). Scanning is performed in constant tunnelling current mode and the tips were mechanically-cut platinum–iridium wires with nominal diameters of 0.4 mm.

2.3. Substrate materials

Mica sheets (Agar Scientific, Essex) are layered crystals with cleavage planes which are atomically flat over several microns. The sheets are mechanically cut to about 1 cm^2, mounted onto a stainless steel disc and cleaved using either a sticky tape or a scalpel. The freshly cleaved mica surface reveals a basal plane covered by K^+ ions (0.57 ions nm^{-2}) [21]. In water some of the K^+ ions dissociate from the surface which results in a negative surface charge density.

Highly oriented pyrolytic graphite (HOPG) was obtained from advanced ceramics. The graphite has atomically flat, micron-square grains, with a layered honeycomb structure and is cleaved by a sticky tape to reveal a fresh layer. The graphite is impermeable, which means that it can be reused after exposure to liquid environments. The negligible outgas rate of the graphite also means that deposition of size-selected clusters onto the graphite can be performed under a high vacuum environment. The HOPG substrates employed were 10 mm × 5 mm.

Flat gold surfaces in the AFM experiments were made using a slightly modified version of Hegner's template-stripping method [22]. Gold was deposited onto freshly cleaved mica surfaces and these were then glued (gold-side down) using a very low viscosity two component, thermally-curable epoxy onto steel disks, which are used for mounting on the AFM tube scanner. The mica is then stripped to reveal the gold surface that mimics the atomically-flat mica surface. The gold films were deposited to thicknesses of 150–200 nm to ensure mechanical stability during subsequent manipulation. The mica can be stripped from these gold surfaces using a combination of chemical treatment and/or mechanical means. Typical surface roughness of gold films prepared by this method is 0.54 nm.

A cluster beam source is used to generate size-selected clusters for pinning on HOPG (see for instance, Carroll *et al* [23–28]). The size-selected clusters are deposited in a circular section of about 3 mm in diameter onto a rectangular graphite substrate (10 mm × 5 mm). The typical deposition time for a sample is 20 min at a current of 2 pA, which results in approximately 1.5×10^9 clusters over the graphite surface. Following the deposition and pinning of the clusters, the samples were stored in an argon atmosphere to minimize oxidation of the clusters. The cluster films are stable not only at room temperature but also at temperatures above 200 °C depending on the pinning energy of the clusters. They are also stable when placed in an autoclave (130 °C for 2 h in high pressure steam) to sterilize the surface.

Figure 8 shows a scanning tunnelling microscope (STM) scan of Au_{55} clusters pinned onto graphite in air. In this example, the size-selected clusters were deposited on the HOPG substrate at 2 pA (i.e. 1.25×10^7 clusters s^{-1}) for 20 min. The pinned gold clusters are stable at room temperature, and are about 4 nm in diameter (including the effects of tip convolution), with a mean height of 0.5 ± 0.1 nm, indicating that the clusters are one or two atomic layers thick.

The two-dimensional platelet morphology of the clusters has been predicted by molecular dynamics simulations [29]. The clusters are randomly distributed over the surface, with an estimated nearest neighbour spacing of 25 ± 10 nm. Using a series of STM scans over different areas of the graphite, the average number of clusters per micron square is about 600, which translates to about 5×10^9 clusters deposited within a 3 mm^2 area on the graphite substrate. Some variation in cluster density (controlled by the cluster beam deposition time) is expected in different samples due to the alignment and focusing properties of the ion beam.

2.4. Protein reconstitution

GroEL was obtained from Sigma-Aldrich (Poole, UK). The proteins were provided in a lyophilized powder form, and stored between 2 and 8 °C. The chaperonin GroEL was then reconstituted at a concentration of 0.01 mg ml^{-1} in a buffer solution containing 50 mM Tris, 150 mM KCl, 10 mM $MgCl_2$, 1 mM dithiothreitol (DTT), and 2.5% (w/v) trehalose at a pH of 7.5. Approximately 50 μl of this solution was pipetted onto the substrate. Where necessary, after incubation at room temperature for 30 min, the sample may be rinsed with an imaging buffer (50 mM HEPES, 50 mM KCl, and 10 mM $MgCl_2$ at a pH of 7.5) as prescribed by Viani *et al* [30]. Imaging was performed in this same buffer, with more ultrapure water being added with time to compensate for evaporation. The sample was left to reach thermal equilibrium

for 30 min before commencement of imaging in the AFM. A fresh solution of the protein was prepared for each experiment.

3. Results and discussion

3.1. GroEL on mica

Mica is often the traditional substrate for AFM studies of protein adsorption. Its negatively-charged surface in liquid implies that many biological molecules can be easily attracted by electrostatic interactions and thus immobilized for probing by the AFM.

When a sub-monolayer concentration of GroEL is deposited on the mica surface, contact mode AFM in buffer solution yields figure 2(a). In this image bright spots corresponding to individual GroEL rings can be observed. However, despite applying the minimum possible force without the cantilever losing contact with the surface, the scan is unstable due to the lateral movement of the protein as the AFM tip sweeps along, producing typical 'scan stripes'. This situation is therefore not conducive to high resolution imaging of the GroEL ring, but it does suggest that the interactions between protein and substrate are relatively weak.

The most common method of stabilizing the GroEL ring on the surface is to increase the concentration of the protein so that at least a monolayer and possibly a multilayer film is formed on the surface. In these conditions, the protein–protein lateral interactions are often sufficient for the AFM scan to yield a stable image such as in figure 2(b). In this image, the bright spots are between 15 and 18 nm in size, close to the expected diameter of the native GroEL ring. This area can be scanned repeatedly without significant changes to the protein film. If the scan is zoomed into a selected area of figure 2(b), the 5 nm internal cavity of the GroEL ring (where protein folding takes place) can be clearly distinguished (figure 2(c)). This clearly implies that the spatial resolution in this AFM image is better than 5 nm, which arises when small asperities at the end of the AFM tip (typically about 2 nm on oxide sharpened silicon nitride tips) perform the scan. The presence of such asperities is commonly exploited for high resolution imaging of membrane proteins [8].

3.2. GroEL on graphite (HOPG)

When GroEL is deposited on the bare graphite surface in buffer solution, the AFM scans (figure 3(a)) reveal: (a) discrete circular spots between 20 and 25 nm in diameter distributed randomly over the surface and (b) larger spots between 60 and 100 nm in diameter located at the step edges of the graphite. The latter behaviour is attributable to the smooth nature of the graphite surface, which enables ready lateral diffusion of the protein at least in the presence of solution. The GroEL rings are thus likely to bind and agglomerate at the more reactive (hydrophilic) binding sites provided by steps or grain boundaries, or the occasional surface point defect.

The monomodal 22 ± 3 nm discrete circular spots are dispersed randomly over the graphite surface, with a nearest neighbour spacing of about 40 nm. Although the size of these spots is relatively close to the expected 15 nm diameter of an individual GroEL ring (as determined on the mica substrate), the measured height of the features is about 3 nm. This discrepancy from the expected height of a double GroEL ring

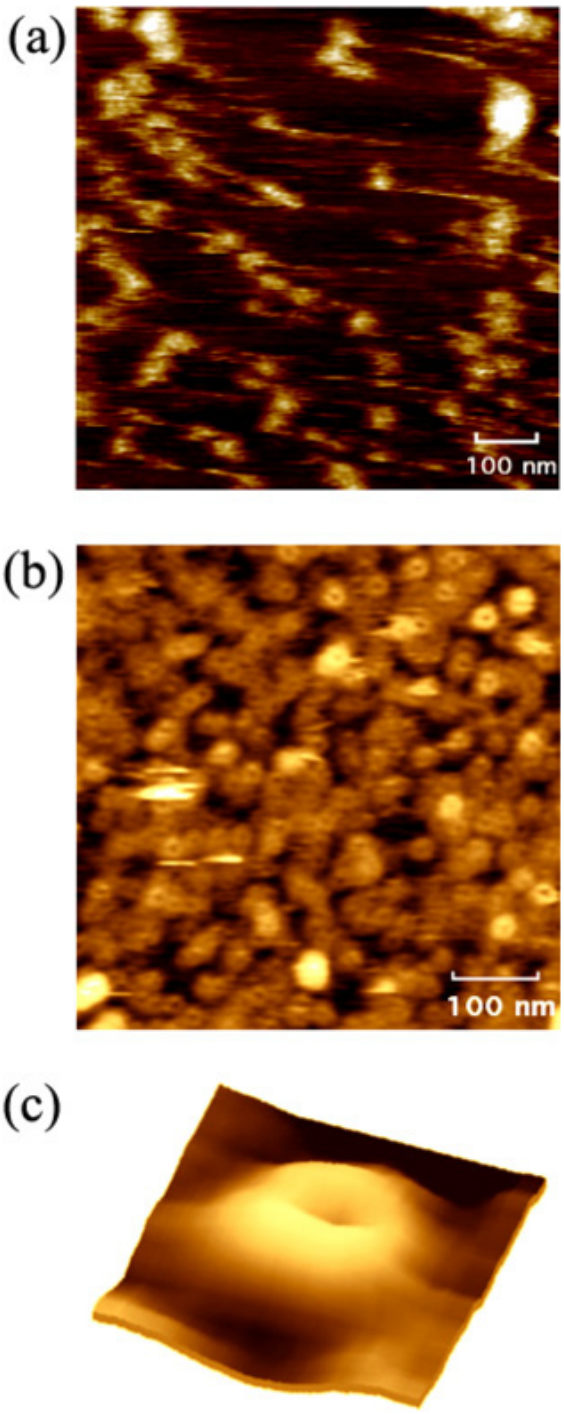

Figure 2. Contact mode AFM scan in buffer solution of GroEL deposited on the mica surface. (a) The protein can be observed, but the image is unstable with 'scan stripes' corresponding to proteins displaced by the tip. (b) Contact mode AFM scan of a densely packed GroEL film deposited on mica. The GroEL rings are uniformly distributed over the surface while the lateral interactions between neighbouring proteins stabilizes the AFM scan so that high resolution images can be obtained. (c) An enhanced section (25 nm × 25 nm) from the original image with the annular shape of the GroEL ring clearly resolved.

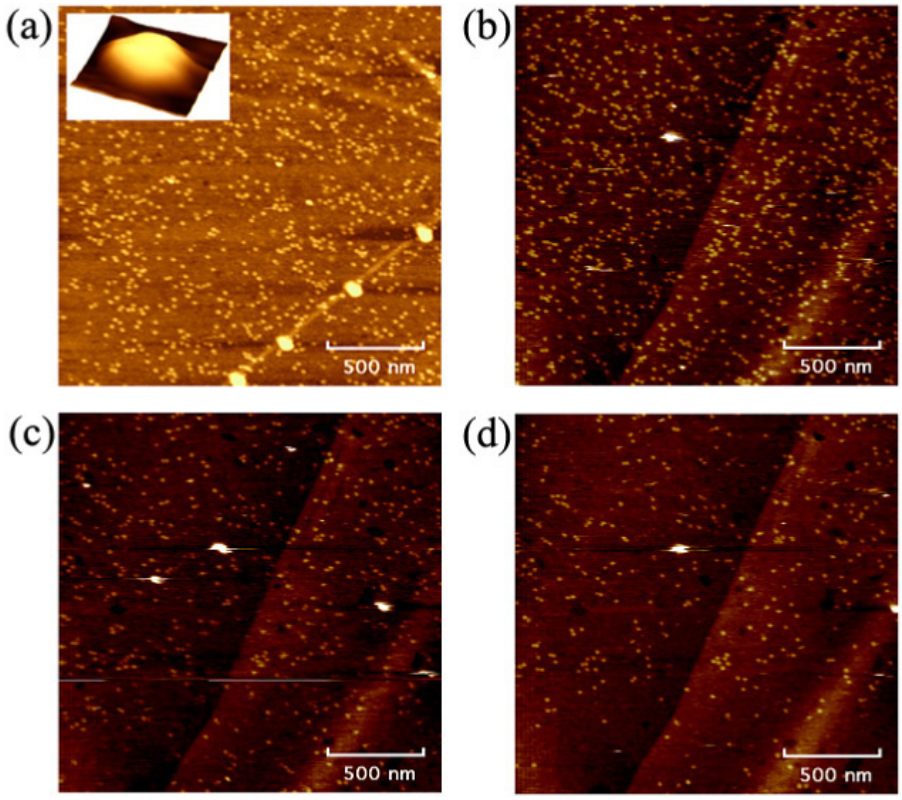

Figure 3. GroEL imaged on the surface of HOPG by contact mode AFM in liquid. (a) At sub-monolayer concentrations of the protein, two distinctive populations can be observed: large islands corresponding to agglomerates of the protein, and smaller spots corresponding to individual GroEL rings. Inset: 40 nm × 40 nm enlarged section from the original image showing an isolated GroEL ring. ((b)–(d)) A sequence of consecutive scans on the graphite surface decorated with GroEL. The protein can be seen to be progressively swept away by the rastering AFM tip. The images were collected at approximately 4 min intervals.

(14 nm) lying flat on the surface, even when compression of the protein by the AFM tip is taken into account, can be explained if the GroEL double rings are bisected into single rings by the scanning AFM tip. The resultant height of the GroEL (single) ring is effectively halved to about 7 nm [15], before AFM tip compression effects. The internal cavity of the GroEL ring was not visible on the graphite surface, unlike mica, suggesting that detailed conformational changes have occurred within the protein.

The possibility of different protein adsorption on the hydrophobic graphite substrate as compared with the hydrophilic mica is well documented in the literature. For instance, Schiener *et al* [18] found that single rings of GroEL prefer to bind to mica via the apical domains whereas on HOPG, the GroEL single rings bind via the equatorial domains. Moreover, other studies have also shown that proteins may adopt different conformations when exposed to the graphite surface (e.g. fibrinogen [3, 5], antifreeze glycoproteins [6]). For these proteins (including GroEL which contains extensive hydrophobic regions), hydrophobic residues which are normally buried within their structure can be exposed to the graphite surface with the molecule lying rather flat on the surface. When scanned by the AFM, these conformational changes result in a drastic decrease in the measured height accompanied by an increase in the lateral dimensions as the protein spreads out over the hydrophobic surface.

When the surface in figure 3(b) is scanned repeatedly by the AFM tip, the GroEL rings are gradually displaced, as illustrated in the sequence of consecutive scans (figures 3(b)–(d)). Although isolated GroEL rings can be moved by the scanning AFM tip in contact mode, they are generally much more stable on the graphite surface as compared with the mica surface at the sub-monolayer concentrations where stabilizing lateral interactions are absent (see for example figure 2(a)). However, we note that the increased interaction between the GroEL ring and the surface can also lead to the distortion of the GroEL ring.

3.3. GroEL on a planar gold film

As compared with the planar surfaces discussed above, a clean evaporated gold film is less hydrophilic than mica, but not as hydrophobic as HOPG. A typical AFM image of such a gold film prepared by evaporation and template stripping is shown in figure 4(a). The measured RMS surface roughness of the film is 1.35 nm, which is sufficiently flat to distinguish large proteins such as the GroEL ring by AFM. Figure 4(b) shows the AFM image in buffer solution when GroEL is deposited at roughly monolayer concentration on the gold film. We see a random distribution of bright spots of about 20 nm in diameter and 6 nm in height populating the surface of the gold film that can be attributed to GroEL rings. In addition

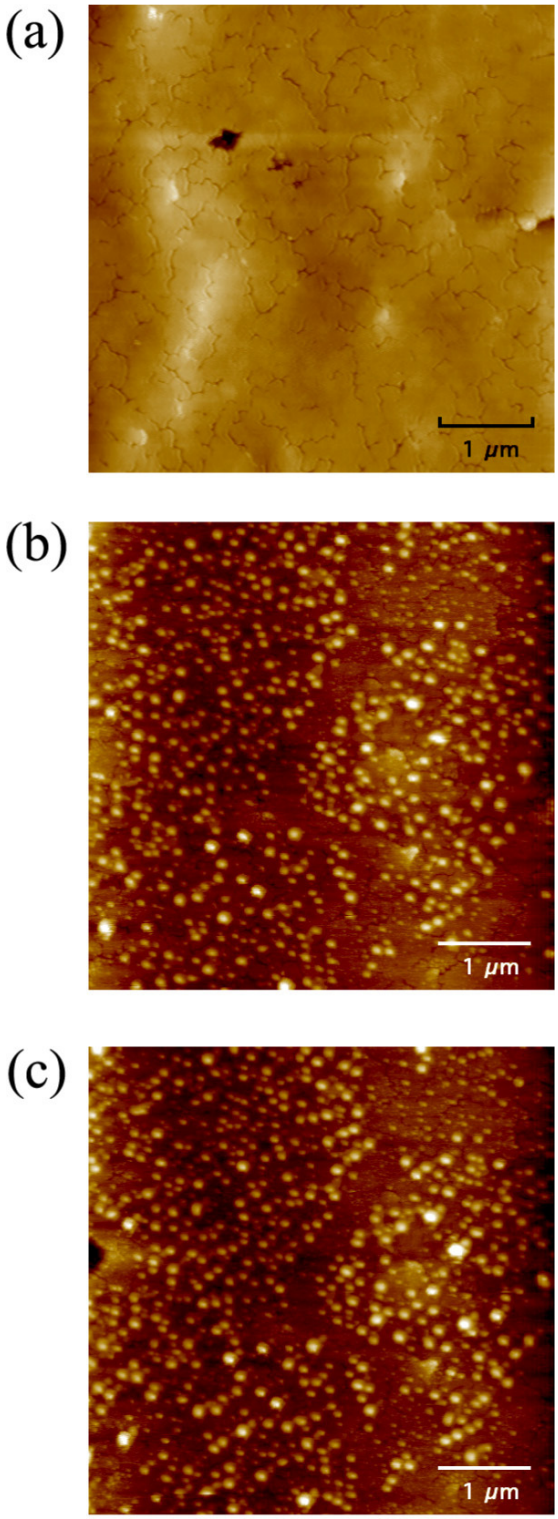

Figure 4. GroEL at monolayer concentration deposited onto the template-stripped gold film and imaged by contact mode AFM in liquid. (a) A template-stripped gold film imaged by contact mode AFM in air. Scan area is 5 μm × 5 μm, and the RMS surface flatness of 1.35 nm. (b) The bright spots can be attributed to GroEL molecules, and are stable against repeated imaging by the scanning AFM tip. The surface has been washed repeatedly by buffer solution prior to imaging. (c) The same area approximately half an hour of repetitive contact mode scans shows the GroEL rings and islands still intact on the extended gold surface.

to these features, we also see much larger spots which can measure above 60 nm in diameter and exceed 16 nm in height. These larger spots, or GroEL 'islands', are also apparent on the graphite surface even at sub-monolayer concentrations of the protein (see figure 3(a)), suggesting that protein island formation is not simply concentration dependent. When the tip is scanned repeatedly over the same area, the GroEL rings and GroEL islands remain stable, in contrast to the previous cases (on HOPG or mica) where the molecules were swept aside by the AFM tip. The internal cavity of the GroEL is not visible in any of the images scanned, which suggests the likelihood that the protein undergoes conformational changes when exposed to the gold surface. We note that the distortion of GroEL rings on extended gold surfaces has been observed before, for instance by Tang *et al* [31].

In contrast to graphite which is relatively inert, a gold surface can form covalent bonds with sulfur-containing cysteine residues in a protein molecule. The covalent binding of proteins to gold surfaces is well documented in the literature. In some instances proteins were nevertheless found to retain their biological activity while immobilized on the surface [32–34]. As each subunit in the GroEL molecule contains 3 cysteine residues, a total of 21 cysteines in a single GroEL ring can potentially bind in a covalent manner to the gold film. The strength of the gold–sulfur bond, about 2 eV [35], suggests that covalent bonds can provide sufficient stability to the immobilized GroEL molecules that they are not displaced by the scanning AFM tip. The stability of the AFM images in figures 3(b) and (c) is a strong indication that cysteine to gold covalent bonds immobilize the GroEL molecules effectively as repetitive AFM scanning is now possible which clearly differs from the cases of GroEL on mica (immobilization via hydrophilic interactions) and on graphite (immobilization via hydrophobic interactions).

3.4. GroEL on size-selected gold clusters

The decoration of the graphite surface with an array of pinned gold nanoclusters dramatically changes the behaviour of the surface with respect to the adsorption of proteins. Contact mode AFM imaging of a gold cluster film in GroEL buffer solution generates figure 5(a), a dispersed array of protein islands with diameters between 15 and 130 nm, which can be assigned to the nucleation of protein islands on the gold clusters dispersed over the surface. The 5 nm cavity in the middle of the chaperonin ring was again missing in the smallest features attributed to individual GroEL rings (15–20 nm in diameter, and 3–4 nm in height). These features sizes are comparable with the GroEL rings deposited onto the extended gold film (see figures 4(b), 3(c)). Since the chaperonin ring contains so many (21) cysteine residues (but no disulfide bridges), we can speculate that on both the extended gold film and the gold clusters the protein is chemisorbed via one or more surface thiolate bonds, hence conferring the observed stability of the protein molecules under repeated contact AFM imaging.

The presence of protein islands larger than a single GroEL ring suggests the formation of protein–protein complexes

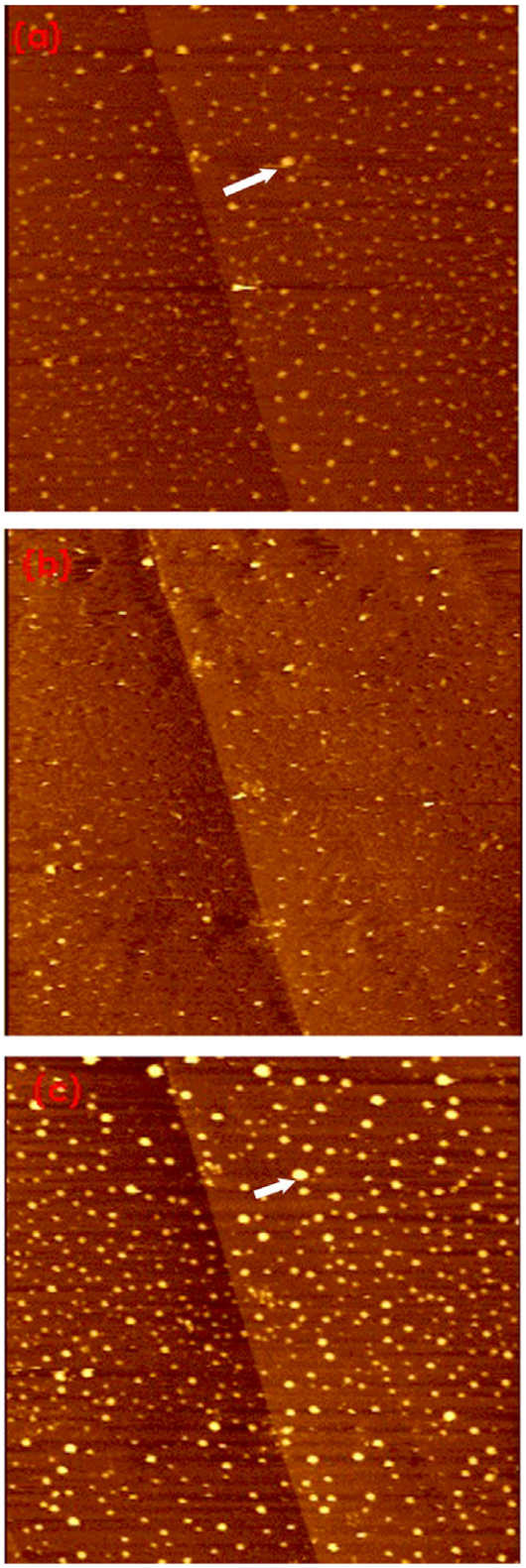

Figure 5. AFM of GroEL onto a graphite nanostructured surface decorated with Au_{55} clusters. (a) GroEL islands and rings immobilized by the gold clusters in imaging buffer solution at pH 7.5. (b) Same scan area as in (a) shortly after addition of excess 1 molar concentration KCl. (c) Same scan area as in (a), approximately 10 min after the addition of excess KCl. The white arrows point to matching sites in (a) and (c). The graphite step is visible at the same location in all the scans. All scans were performed at 4 μm $\times$ 4 μm.

around one (or more) GroEL monomer(s) anchored by gold cluster(s). Thus, we investigate further the formation of the GroEL islands via the *in situ* addition of electrolytes to modulate the strength of the electrostatic interactions between charged groups in different protein molecules. Such addition of salts can affect the conformational stability of proteins via intramolecular charge–charge interactions, but it also tends to prevent aggregate formation via intermolecular electrostatic interactions. We note that the GroEL ring itself is very robust even under extreme conditions of high temperatures (up to 75 °C) and high salt concentrations [36].

When an excess solution of KCl at 1 molar concentration is introduced *in situ*, the AFM now yields figure 5(b), where most of the protein islands are still present, but appear to be smaller in size. Thus it seems that most of the nucleus molecules in the islands (i.e. the protein molecules chemisorbed on the gold clusters) remain intact. The implication of these observations is twofold: (a) the attraction between the nucleus GroEL molecule and other molecules forming the large islands is electrostatic and can be disrupted by the presence of excess electrolytes, and (b) since the nucleus molecules are not much affected by the presence of electrolytes, the bond with the underlying gold cluster is plausibly covalent in nature. 10 min after the introduction of the salt solution, the AFM yields figure 5(c) where the protein islands have been recondensed at largely the same locations, as in figure 5(a). The reversibility of the process is a strong indication that the GroEL islands are formed by electrostatic (and not hydrophobic) interactions.

The dynamics of the process of dissolution and recondensation of the protein islands is illustrated by the size distributions in figure 6. The number and size of GroEL islands falls rapidly when excess KCl is first injected, dropping to about a third of its original value (figure 6(b)), while the peak of the size distribution shifts from about 80 to 60 nm. Within 10 min of the injection, however, about 70% of the GroEL islands have been recovered (figure 6(c)), and the size distribution of the islands is now closer to the original state. After about 20 min, more than 80% of the islands have been recovered while the size distribution of the islands appears to skew towards larger diameter, suggesting that some alterations in the arrangement of the GroEL islands do occur during and after the injection of KCl.

It has already been established in previous work that the presence of surface accessible cysteine residues is important for protein immobilization by gold nanoclusters (see for example [37–40]). To determine whether the cysteine residues (and the sulfur atoms therein) are present on the surface of the GroEL to bind to the gold clusters, we have computed the molecular surface areas of the cysteine residues of the quaternary GroEL ring structure and an individual GroEL molecule.

Table 1 shows the results of an analysis of the GroEL structure using a molecular surface area (MSA) package (SurfRace [41]). The analysis of an undistorted GroEL heptameric ring (single ring) shows no sulfur atoms are exposed at any of the cysteine residues, although some parts of the cysteine backbones are on the molecular surface of the

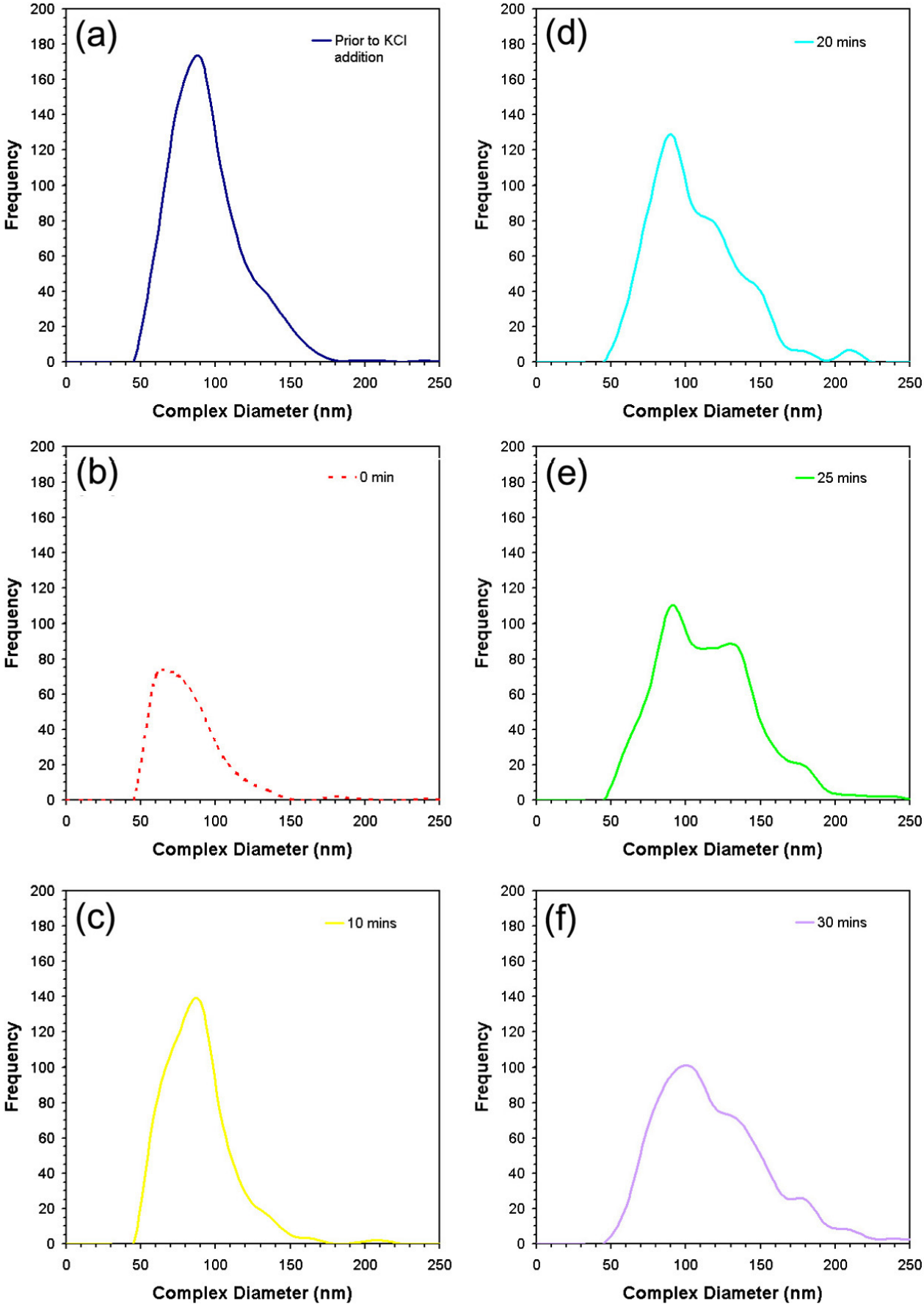

Figure 6. Evolution of the size distribution of GroEL islands at selected time intervals when excess KCl is injected. Data extracted from AFM scans using image SXM [20].

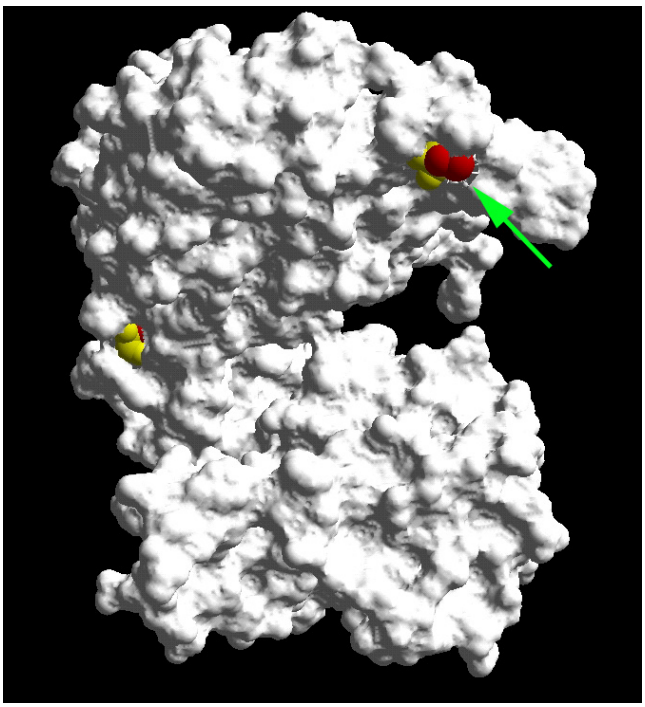

Figure 7. Composite molecular surface—van der Waals' surface of Chain A of the GroEL ring. The side chains of the cysteine are coloured red (online), while the amino acid backbone is yellow (online). The arrow (green online) points to Cys 519, the most likely binding site for gold nanoclusters based on the MSA analysis.

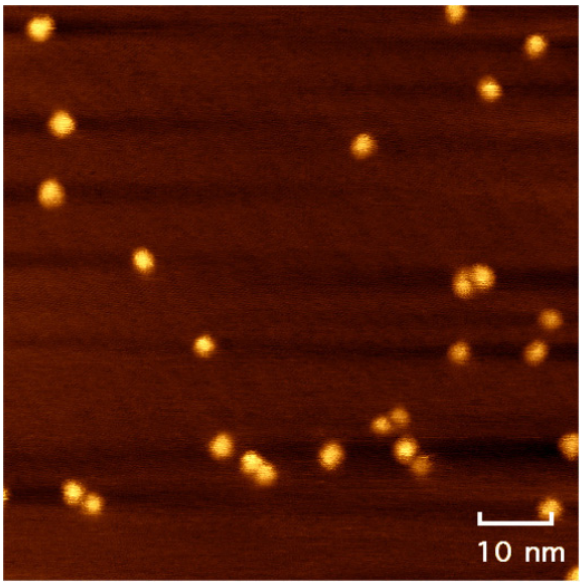

Figure 8. STM scan of Au_{55} clusters on graphite, with the graphite steps visible across the image (80 nm × 80 nm). Image was collected at a constant tunnelling current of 0.4 nA, and a tip bias voltage of 0.4 V.

Table 1. GroEL (heptamer and one subunit in isolation) analysed by SurfRace [41]. The numbers in square brackets denote the residues which form disulfide bridges within the protein.

Protein	PDB ID	Cys residue	Total MSA	Sulfur MSA	Will bind to Au clusters?
GroEL (heptamer)	1OEL	138	18.33	0.00	No
		458	11.72	0.00	
		519	0.00	0.00	
GroEL (one subunit)	1OEL (Chain A)	138	20.90	0.00	Yes
		458	16.67	0.00	
		519	48.48	15.16	

protein. However, if the constituent subunits of the GroEL are investigated separately (e.g. by examining Chain A in isolation so that the subunits are no longer considered to be interfacing with each other), then the sulfur atom of Cys 519 becomes readily available. The exposed and convex molecular surface area of the sulfur measures about 15 $Å^2$ and is illustrated in figure 7. The exposure of the cysteines of the GroEL ring may thus be possible if the ring distorts to accommodate the surface, as we seem to observe on graphite or the extended gold film. Of course the formation of a covalent bond between protein and surface would itself add to the driving force for the distortion of the protein complex on the solid surface.

4. Conclusions

Adsorption of the large GroEL protein complex on surfaces has been studied by contact mode AFM in aqueous environments (buffer solution). The 5 nm internal cavity of the protein is large enough to be resolved by AFM, providing useful structural information about the conformation of the model GroEL on surfaces. On hydrophilic mica, the GroEL ring essentially retains its native conformation and can be imaged at high resolution, while on the hydrophobic graphite substrate (HOPG), the internal cavity of the GroEL ring is no longer visible in the AFM scans, suggesting that the protein may undergo conformational changes to accommodate the nature of the graphite surface. GroEL deposited onto an extended gold surface can be imaged repeatedly without disturbance as cysteine residues within the protein are believed to form strong covalent bonds to the gold surface. However, unlike mica and HOPG, large GroEL islands are also observed on the planar gold film.

On a nanostructured surface composed of size-selected gold clusters pinned on graphite, AFM scans in solution reveal the adsorption of GroEL rings as well as the formation of large GroEL islands. The strength of adsorption between protein and cluster, as revealed by the AFM scans in contact mode cannot be simply due to hydrophilic interactions. As with the extended gold surface, surface thiolate bonds can be formed between the cysteines of the GroEL ring and the gold nanoclusters. When excess electrolyte is injected into the solution, the GroEL islands tend to shrink and decrease in number before recondensation of islands primarily at the same surface sites, suggesting that the GroEL islands are produced by chemisorbed molecules which act as nucleation sites for the capture of further molecules via electrostatic interactions.

In this topical review of the adsorption of a model protein molecule, GroEL, we have been able to demonstrate the range

of behaviour which appears when protein molecules interact with solid surfaces in the solution environment best designed to maintain protein function. Such studies should lead to a better understanding of the protein adsorption mechanism, as relevant both to fundamental biophysical processes and applications, e.g. in protein biochips and microfluidics.

References

[1] Engel A *et al* 1995 Functional-significance of symmetrical versus asymmetrical Groel–Groes chaperonin complexes *Science* **269** 832–6

[2] Xu Z H, Horwich A L and Sigler P B 1997 The crystal structure of the asymmetric GroEL–GroES–(ADP)(7) chaperonin complex *Nature* **388** 741–50

[3] Agnihotri A and Siedlecki C A 2004 Time-dependent conformational changes in fibrinogen measured by atomic force microscopy *Langmuir* **20** 8846–52

[4] Cullen D C and Lowe C R 1994 Afm studies of protein adsorption.1. Time-resolved protein adsorption to highly oriented pyrolytic-graphite *J. Colloid Interface Sci.* **166** 102–8

[5] Marchin K L and Berrie C L 2003 Conformational changes in the plasma protein fibrinogen upon adsorption to graphite and mica investigated by atomic force microscopy *Langmuir* **19** 9883–8

[6] Sarno D M *et al* 2003 Direct observation of antifreeze glycoprotein-fraction 8 on hydrophobic and hydrophilic interfaces using atomic force microscopy *Langmuir* **19** 4740–4

[7] Ellis J S *et al* 2004 Direct atomic force microscopy observations of monovalent ion induced binding of DNA to mica *J. Microsc.* **215** 297–301

[8] Muller D J *et al* 1999 Electrostatically balanced subnanometer imaging of biological specimens by atomic force microscope *Biophys. J.* **76** 1101–11

[9] Kirby A R *et al* 1996 Visualization of plant cell walls by atomic force microscopy *Biophys. J.* **70** 1138–43

[10] Bushell G R *et al* 1995 Imaging and nano-dissection of tobacco mosaic-virus by atomic-force microscopy *J. Microsc.* **180** 174–81

[11] Brayshaw D J, Berry M and McMaster T J 2003 Optimisation of sample preparation methods for air imaging of ocular mucins by AFM *Ultramicroscopy* **97** 289–96

[12] McMaster T J *et al* 1999 Atomic force microscopy of the submolecular architecture of hydrated ocular mucins *Biophys. J.* **77** 533–41

[13] Costa L T *et al* 2004 Chemical treatment of mica for atomic force microscopy can affect biological sample conformation *Biophys. Chem.* **109** 63–71

[14] Valle F *et al* 2001 Imaging the native structure of the chaperone protein GroEL without fixation using atomic force microscopy *J. Microsc.* **203** 195–8

[15] Valle F *et al* 2002 AFM structural study of the molecular chaperone GroEL and its two-dimensional crystals: an ideal 'living' calibration sample *Ultramicroscopy* **93** 83–9

[16] Mou J X *et al* 1996 High resolution surface structure of E-coli GroES oligomer by atomic force microscopy *Febs Lett.* **381** 161–4

[17] Mou J X *et al* 1996 Chaperonins GroEL and GroES: views from atomic force microscopy *Biophys. J.* **71** 2213–21

[18] Schiener J *et al* 2005 How to orient the functional GroEL-SRI mutant for atomic force microscopy investigations *Biochem. Biophys. Res. Commun.* **328** 477–83

[19] Engel A and Muller D J 2000 Observing single biomolecules at work with the atomic force microscope *Nat. Struct. Biol.* **7** 715–8

[20] Barrett S D 2005 http://www.ImageSXM.org.uk cited

[21] Muller D J, Amrein M and Engel A 1997 Adsorption of biological molecules to a solid support for scanning probe microscopy *J. Struct. Biol.* **119** 172–88

[22] Hegner M, Wagner P and Semenza G 1993 Ultralarge atomically flat template-stripped Au surfaces for scanning probe microscopy *Surf. Sci.* **291** 39–46

[23] Carroll S J *et al* 1998 Deposition and diffusion of size-selected (Ag − 400(+)) clusters on a stepped graphite surface *Appl. Phys.* A **67** 613–9

[24] Carroll S J *et al* 2000 Pinning of size-selected Ag clusters on graphite surfaces *J. Chem. Phys.* **113** 7723–7

[25] Pratontep S *et al* 2005 Size-selected cluster beam source based on radio frequency magnetron plasma sputtering and gas condensation *Rev. Sci. Instrum.* **76** 045103

[26] von Issendorff B and Palmer R E 1999 A new high transmission infinite range mass selector for cluster and nanoparticle beams *Rev. Sci. Instrum.* **70** 4497–501

[27] Goldby I M *et al* 1996 Diffusion and aggregation of size-selected silver clusters on a graphite surface *Appl. Phys. Lett.* **69** 2819–21

[28] Palmer R E, Pratontep S and Boyen H G 2003 Nanostructured surfaces from size-selected clusters *Nat. Mater.* **2** 443–8

[29] Pratontep S *et al* 2003 Scaling relations for implantation of size-selected Au, Ag, and Si clusters into graphite *Phys. Rev. Lett.* **90**

[30] Viani M B *et al* 2000 Probing protein–protein interactions in real time *Nat. Struct. Biol.* **7** 644–7

[31] Tang S L and McGhie A J 1996 Imaging individual chaperonin and immunoglobulin G molecules with scanning tunneling microscopy *Langmuir* **12** 1088–93

[32] Andolfi L *et al* 2003 Scanning probe microscopy characterization of gold-chemisorbed poplar plastocyanin mutants *Surf. Sci.* **530** 181–94

[33] Andolfi L *et al* 2002 A poplar plastocyanin mutant suitable for adsorption onto gold surface via disulfide bridge *Arch. Biochem. Biophys.* **399** 81–8

[34] Friis E P *et al* 1997 Dynamics of Pseudomonas aeruginosa azurin and its Cys3Ser mutant at single-crystal gold surfaces investigated by cyclic voltammetry and atomic force microscopy *Electrochim. Acta* **42** 2889–97

[35] Grandbois M *et al* 1999 How strong is a covalent bond? *Science* **283** 1727–30

[36] Kusmierczyk A R and Martin J 2000 High salt-induced conversion of Escherichia coli GroEL into a fully functional thermophilic chaperonin *J. Biol. Chem.* **275** 33504–11

[37] Leung C *et al* 2004 Immobilisation of protein molecules by size-selected metal clusters on surfaces *Adv. Mater.* **16** 223–6

[38] Prisco U *et al* 2005 Residue-specific immobilisation of protein molecules by size-selected clusters *J. R. Soc. Interface* **1** 169–75

[39] Palmer R E and Leung C 2007 Immobilisation of proteins by atomic clusters on surfaces *Trends Biotechnol.* **25** 48–55

[40] Collins J A *et al* 2004 Clusters for biology: immobilisation of proteins by size-selected metal clusters *Appl. Surf. Sci.* **226** 197–208

[41] Tsodikov O V, Record M T and Sergeev Y V 2002 Novel computer program for fast exact calculation of accessible and molecular surface areas and average surface curvature *J. Comput. Chem.* **23** 600–9

[42] Guex N and Peitsch M C 1997 SWISS-MODEL and the Swiss-PdbViewer: an environment for comparative protein modeling. *Electrophoresis* **18** 2714–23